Wind and Structures, Vol. 10, No. 4 (2007) 347-366
DOI: http://dx.doi.org/10.12989/was.2007.10.4.347

Estimating peak wind load effects in guyed masts

B. F. Sparling† and L. D. Wegner‡

Department of Civil Engineering, University of Saskatchewan, 57 Campus Drive, Saskatoon, SK, S7N 5A9, Canada

(Received August 1, 2005, Accepted July 10, 2007)

Abstract. Guyed masts subjected to turbulent winds exhibit complex vibrations featuring many vibration modes, each of which contributes to various structural responses in differing degrees. This dynamic behaviour is further complicated by nonlinear guy cable properties. While previous studies have indicated that conventional frequency domain methods can reliably reproduce load effects within the mast, the system linearization required to perform such an analysis makes it difficult to relate these results directly to corresponding guy forces. As a result, the estimation of peak load effects arising jointly from the structural action of the mast and guys, such as leg loads produced as a result of guy reactions and mast bending moments, is uncertain. A numerical study was therefore undertaken to study peak load effects in a 295 m tall guyed mast acted on by simulated turbulent wind. Responses calculated explicitly from nonlinear time domain finite element analyses were compared with approximate methods in the frequency domain for estimating peak values of selected responses, including guy tension, mast axial loads and mast leg loads. It was found that these peak dynamic load effects could be accurately estimated from frequency domain analysis results by employing simple, slightly conservative assumptions regarding the correlation of related effects.

Keywords: guyed mast; dynamic analysis; wind engineering; finite element analysis; frequency domain analysis; time domain analysis; peak load effects.

1. Introduction

Guyed masts used to support and elevate telecommunication equipment rank among the tallest manmade structures, with some exceeding 600 m in height. The slenderness of the mast, combined with the sag inherent in the supporting guy cables, results in an exceptionally flexible structure prone to large scale vibrations in gusty winds.

Strong dynamic interaction between the slender mast and the numerous, relatively massive guys generates complex vibration patterns when the system is excited by random turbulence. Unlike conventional building structures that exhibit relatively few dominant vibration modes, guyed masts typically feature anywhere between ten and twenty active modes (Sparling 1995). As illustrated in Fig. 1, the lower modes typically feature large amplitude oscillations of the slackened leeward guys at various levels and dominate the displacement response of the mast, while higher modes are characterised by mast vibrations of increasing complexity and so contribute primarily to the mast

† Corresponding Author, E-mail: bruce.sparling@usask.ca

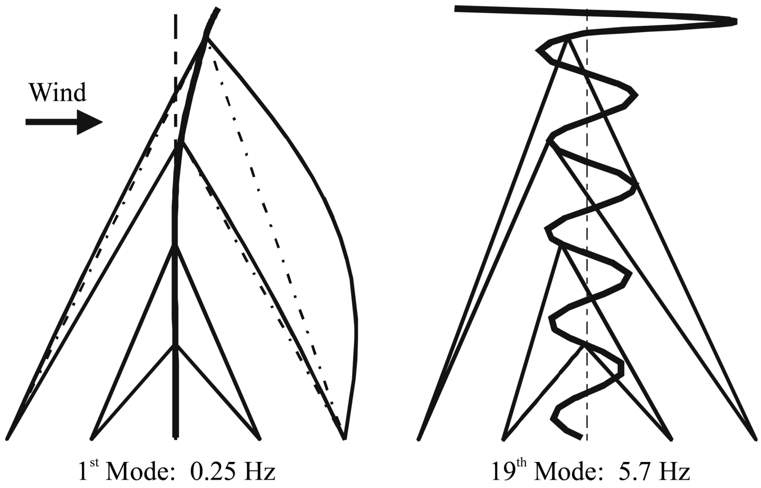

Fig. 1 Example guyed mast vibration modes (note: the scaling of the mode shapes shown is arbitrary and chosen purely for the purposes of illustration)

bending moments and shear forces (Davenport and Vickery 1968).

Each of the active modes contributes in varying degrees to an assortment of structural responses at different locations on the mast. Adding to the overall complexity, critical load effects can arise from the combined actions of two or more primary structural responses. For example, leg loads in a lattice mast structure are generated jointly by axial forces and bending moments within the mast (see Fig. 2), while torsion and direct shear both contribute to diagonal and horizontal member loads. With components of a given load effect originating from different structural actions, each of which is influenced by several vibration modes, dynamic fluctuations of the load effect contributed from different sources tend to be poorly coordinated, making the estimation of the resultant effect somewhat difficult and uncertain.

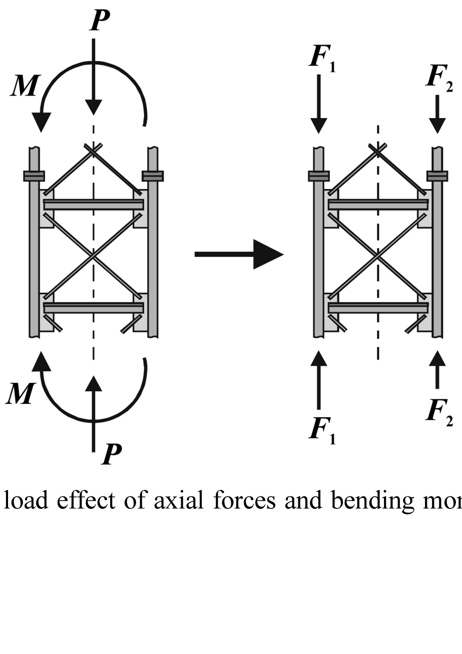

Fig. 2 Combined load effect of axial forces and bending moments in the mast

Another distinguishing feature of guyed masts is their inherently nonlinear behaviour. In addition to the 2nd order (P-Δ) effects associated with displacements of the slender mast, constantly changing levels of sag in the guy cables induce significant variations in the lateral restraint provided to the mast.

The estimation of peak resultant load effects for design purposes can be accomplished directly using time domain analysis methods, in which the response of the guyed mast is determined at a series of successive time steps (Buchholdt, *et al*. 1986, Iannuzzi and Spinelli 1989, Sparling and Davenport 1998). Since the simultaneous values of the primary structural responses are known for each time step, combined load effects can be calculated explicitly and the peak values tracked over the analysis period. In addition, nonlinear system characteristics can be updated continuously based on the current displaced configuration of the system. High computational demands, difficulties involved in handling the large volume of output data, and the requirement for a predefined wind storm time history with realistic spatial and temporal characteristics, however, have limited the practical application of time domain analyses.

In practice, dynamic analyses of guyed masts for wind loading conditions are more commonly performed in the frequency domain using spectral analysis approaches (Davenport 1962, Vellozzi 1975, ASCE 2002). Rather than explicit time histories of individual structural responses, frequency domain methods provide probabilistic descriptions of response statistics, including time-averaged mean values, root-mean-square (*rms*) response levels, and expected peak values.

In the strictest sense, however, the application of frequency domain analysis methods to guyed masts can be questioned in light of their nonlinear structural properties. Significant nonlinearities not only invalidate the principle of response superposition, they also complicate the implementation of eigenvalue solvers that are used as input to the frequency domain calculations. Traditionally, this limitation has been overcome, in part, by considering nonlinear effects in determining the static response of guyed masts to the mean component of the wind loads, while assuming that turbulence induced vibrations occur in a linear manner about the mean position (IASS 1981). Using this approach, Sparling and Wegner (2005) demonstrated that frequency and time domain analysis methods can yield similar response predictions for mast displacements and bending moments as long as the wind loading characteristics assumed for the two methods are comparable.

Although dynamic linearization techniques appear to produce reasonable estimates of overall system response, caution must be exercised when extending this approximation to load effects specifically induced by the nonlinear guy cables. Instantaneous guy tensions, for example, can be influenced significantly by the alternating softening and hardening behaviour experienced as the mast oscillates in response to wind gusts. Axial and lateral loads applied by the guys on the mast will also be affected in a similar manner.

In the frequency domain method, combined load effects generated by two or more primary responses, each featuring the contributions of several vibration modes, must be estimated based on some assumption regarding the degree to which the individual responses are correlated (act in unison) over time. Closed form analytical solutions, including the square-root-sum-of-squares (SRSS) and complete-quadratic-combination (CQC) approaches, are commonly used for this purpose (Chopra 1995). Since these combination methods invariably make use of response superposition in some form, however, their application to nonlinear systems such as guyed masts is somewhat speculative.

In this paper, the results of a numerical study are presented describing the time domain dynamic analysis of a 295 m tall guyed mast subjected to simulated turbulent winds. The primary objective of the study was to investigate dynamic load effects arising from the combined action of two or more partially correlated structural responses, including guy tensions, axial mast loads and mast leg loads, in the presence of significant nonlinear behaviour. The findings represent a contribution toward the establishment of rational guidelines for combining dynamic load effects in guyed masts analysed using frequency domain techniques. Such guidelines would also be informative in the application of various approximate dynamic analysis methods included in recent design standards (CSA 2001, CEN 2006, ANSI/TIA 2005).

2. Overview of frequency domain analysis methods

The time history of a specific response, or load effect, $r(t)$ in gusty wind conditions typically resembles the plot illustrated in Fig. 3(a). Conceptually, this response could represent a wide variety of structural actions including the displacement, shear force or bending moment at some location in the mast, as well as tension in a guy cable. In the frequency domain approach, this response is separated into a time-averaged mean component $\bar{r}$ and a fluctuating dynamic component. As indicated in Fig. 3(a), the fluctuating component may be further subdivided into a slowly varying background response $r_B(t)$ and a more rapidly varying resonant response, $r_R(t)$.

The fluctuating response can be described in terms of its frequency content using a power spectral density function, or power spectrum, $S_r(f)$, the area under which represents the mean-square value of the dynamic response, $\tilde{r}^2$ (where f denotes the frequency in Hz). In Fig. 3(b), the power spectrum has been plotted in the semi-logarithmic form of $f \cdot S_r(f)$ versus $\ln(f)$, which encloses the same area ($\tilde{r}^2$) as the original spectrum, while providing better definition of the response in the low frequency range. As suggested in this plot, response spectra for guyed masts in turbulent winds typically feature a broad hump in the low frequency (background) range, along with a series of narrow, higher frequency resonant peaks centred on the natural frequencies of the structure.

The background component $r_B(t)$ may be characterised as the quasi-static response of the structure to large, slowly varying wind gusts. It is commonly estimated on the basis of a linear static analysis, using a time-averaged broad-band correlation function to account for the lack of spatial correlation in the gusty wind loads (ASCE 2002). Approximate guy stiffness properties for background response calculations are often based on the displaced configuration of the guys at the mean equilibrium position of the mast.

The resonant dynamic response, on the other hand, is typically found in the frequency domain

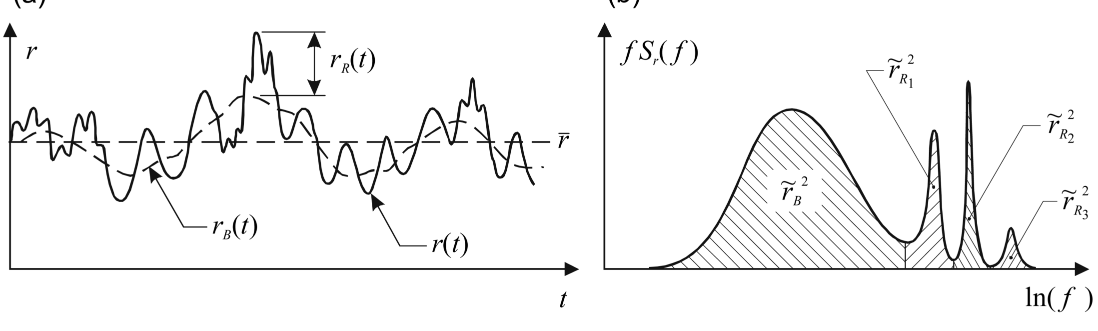

Fig. 3 Representations of wind-induced response: (a) time history; and (b) power spectrum

using conventional modal analysis methods (ASCE 2002). For the requisite eigenvalue analysis, the nonlinear guys must first be replaced by suitable spring-mass-damper representations that exhibit appropriate dynamic characteristics (Kärnä 1984). The resonant component for each response type is then computed individually for all active vibration modes. For structures with low damping and well separated natural frequencies, the resultant *rms* resonant response $\tilde{r}_R$ may then be estimated using the SRSS method:

$$\tilde{r}_R = \sqrt{\sum \tilde{r}_{R_i}} \tag{1}$$

where $\tilde{r}_{R_i}$ is the *rms* resonant response for the *i*th vibration mode. Alternatively, the CQC method may be used to obtain a more accurate estimate of the combined modal response where the assumption of well separated modes is not satisfied.

The peak value $\hat{r}$ of the specific response in question can be estimated from the mean and *rms* components using the expression (Davenport 1962)

$$\hat{r} = \bar{r} \pm g_p \tilde{r} = \bar{r} \pm g_p \sqrt{\tilde{r}_B^2 + \tilde{r}_R^2} \tag{2}$$

in which $\tilde{r}_R$ is the *rms* background response and g_p is a statistical peak factor. As demonstrated by Davenport (1964), the statistical peak factor g_p can be estimated by the expression

$$g_p = \sqrt{2\ln(vT)} + \frac{0.5772}{\sqrt{2\ln(vT)}} \tag{3}$$

where T is the period over which the response is considered (s), the response cycling rate v is

$$v = \sqrt{\frac{\int f^2 S_r(f)\mathrm{d}f}{\int S_r(f)\mathrm{d}f}} \approx \frac{\sqrt{\sum_i f_i^2 \tilde{r}_{R_i}^2}}{\sqrt{\tilde{r}_B^2 + \sum \tilde{r}_{R_i}^2}} \tag{4}$$

and f_i is the *i*th natural frequency. For guyed masts in gusty winds, the peak factor g_p varies over the limited range of approximately 3.0 to 4.25 (Sparling 1995).

As note previously, the dynamic linearization of structural properties that is implicit in Eq. (2) has been found to provide satisfactory estimates of peak dynamic mast displacements, bending moments and shear forces. It remains unclear, though, as to the proper method for generating similar estimates of peak guy responses since the guys themselves exhibit notable nonlinear tendencies during vibration (Sparling, *et al.* 2000). As a result, the combination of partially correlated load effects arising from the actions of both the mast and the guys is, at present, uncertain.

3. Description of the study

3.1. Overview

Dynamic finite element analyses of a selected guyed telecommunication mast were performed in the time domain. The guyed mast was loaded by a numerically generated turbulent wind field acting at two different orientations with respect to the mast.

3.2. Physical characteristics of the guyed mast

An existing 295 m tall guyed mast with four guy support levels was selected for this study. The mast consists of a triangular lattice structure with a face width of 2.3 m and a pinned base connection. A flexible 20 m long antenna is cantilevered above the top of the mast. This guyed mast has been investigated previously both experimentally and analytically (Hartmann and Davenport 1966, Sparling and Davenport 1998, Sparling and Wegner 2005).

Physical properties of the mast are shown schematically in Fig. 4, including the unit weight (w_m), bending stiffness ($E\,I_m$) and effective drag area (i.e. the projected unit face area modified by a drag factor, $C_d\,A$). The geometry and physical properties of the guys under still air conditions are provided in Table 1, where L_c is the straight chord length between the cable ends, θ is the vertical angle between the chord line and the horizontal, a_G is the cross-sectional area, w_G is the unit weight, $\bar{T}$ is the average tension, and E_G is the elastic modulus.

3.3. Time domain finite element model

A schematic of the finite element model for the guyed mast is shown in Fig. 5. The mast was modelled using beam-column elements whose stiffness, mass and drag characteristics reflected the distribution in the physical properties of the prototype, as shown in Fig. 4. Each span of the mast between guy support levels was divided into two equal length elements. One additional element was used to model the cantilevered antenna.

A consistent formulation was employed to generate the resulting stiffness, mass, damping and

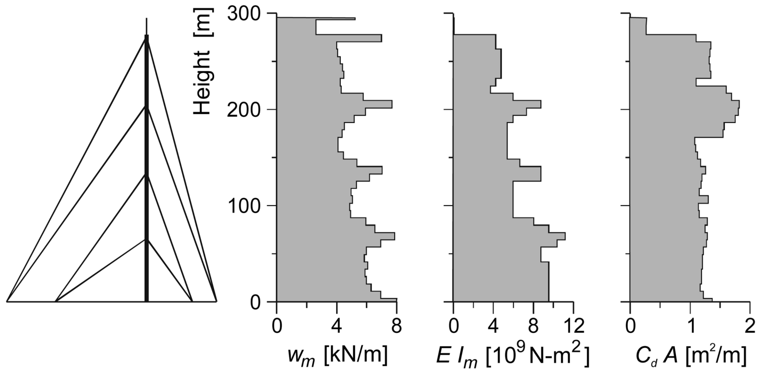

Fig. 4 Description of mast properties

Table 1 Geometry and physical properties of guys

Level	Height [m]	L_c [m]	θ [deg]	a_G [mm^2]	w_G [kN/m]	$\bar{T}$ [kN]	E_G [MPa]
1	65.760	117.100	34.40	723.0	0.057	91.63	165,470
2	134.340	165.810	54.60	955.0	0.075	128.11	165,470
3	204.830	257.100	54.60	1,477.0	0.116	213.52	158,570
4	275.310	316.930	61.70	955.0	0.075	131.67	165,470

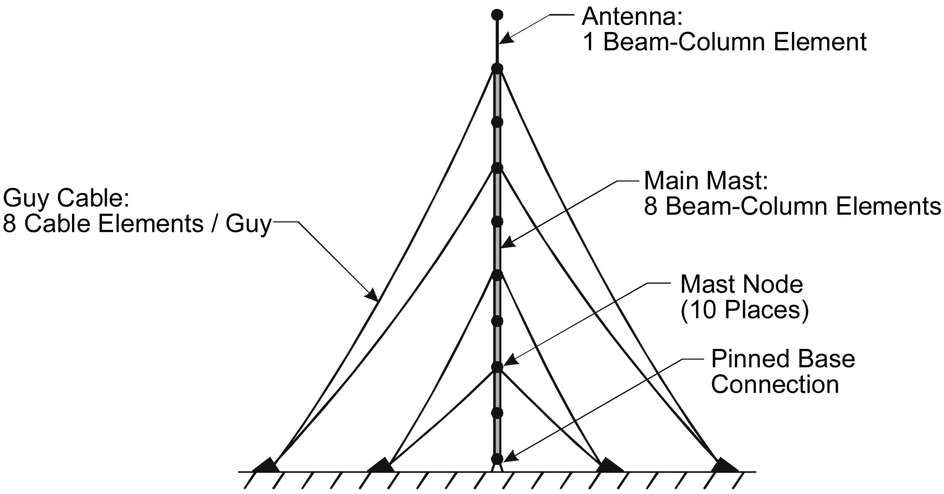

Fig. 5 Schematic of finite element model used in time domain analyses

applied force matrices for the mast elements. Flexural softening (geometric stiffness) effects within individual mast elements due to gravity and guy prestressing axial forces were included. In addition, second-order effects associated with the instantaneous orientation of the mast elements in their current displaced position were also continuously updated during both the static and dynamic phases of the analyses. For the planar analyses considered in this study, each mast node possessed two translational (alongwind and vertical) and one rotational degrees of freedom. Torsional motion of the mast was not considered.

Each guy was modelled using eight equal length cable elements based on a catenary suspended profile. As described in Sparling (1995), an iterative procedure was implemented to calculate cable element stiffness and end force values for each displaced configuration of the guy. Cable mass was divided equally among the elements and lumped at the guy nodes. Since the three dimensional displaced profile of the guys influenced the resulting directional stiffness characteristics at their upper ends, guy nodes were permitted to translate in three orthogonal directions, unlike the planar constraints imposed on the mast. To account for the eccentricity produced by attaching the guy to a leg of the mast, the top guy node was connected to the appropriate mast node by a fictitious, rigid horizontal arm radiating out from the mast centreline to the guy attachment point.

The time domain analyses were carried out in two stages. First, an iterative solution was performed to determine the nonlinear static response of the system to mean wind loads. A step-by-step integration of the governing equations of motion was subsequently used to calculate the dynamic response to wind gust loading. Newmark's β method, assuming constant-average acceleration, was selected as the time marching scheme (Bathe and Wilson 1976). During this phase, system property matrices were continuously updated to reflect the current displaced position. In addition, an iterative Newton-Raphson procedure was implemented to enforce dynamic equilibrium at the end of each time step (Sparling 1995).

The time domain studies were conducted over a simulated time period of 800 s. To avoid consideration of the initial transient response as the system was accelerated from rest, only the final 600 s (approximately 120 times the fundamental period of the guyed mast) were considered in subsequent analyses. A constant time step increment of $\Delta t = 0.0488281\text{s}$ was adopted throughout, satisfying the criteria that $\Delta t \leq T_{min}/10$, where T_{min} is the period corresponding to the highest significant frequency content of the turbulent wind (roughly 2 Hz). This increment also generated exactly $3 \cdot 2^{12}$ time steps within the 600 s period under consideration, facilitating the Fast Fourier Transform (FFT) analysis of response data.

A proportional (Rayleigh) formulation was used to represent all structural damping (Chopra 1995). Since this type of damping is inherently frequency dependent, the relevant parameters were defined in such a way so that structural damping remained as close as possible to the target 0.5% of critical damping over the frequency range corresponding to the active modes for this particular mast. Aerodynamic damping was calculated explicitly at each time step (Sparling and Davenport 1998).

3.4. Simulated wind conditions

The instantaneous wind velocity $U(z, t)$ at some height z above the base of the mast was assumed to consist of two components: a steady mean (time-averaged) component $\overline{U}(z)$, and a horizontal turbulent component $u(z, t)$ acting in the mean wind direction. The mean wind speed was defined by the logarithmic profile:

$$\overline{U}(z) = \overline{U}_{10}\frac{\ln(z/z_o)}{\ln(10/z_o)} \tag{5}$$

where $\overline{U}(z)$ is the reference wind speed at an elevation of 10 m, and z_o is the characteristic roughness length for the site. To emphasise the role of turbulence in this study, $\overline{U}_{10}$ was taken to be 22.0 m/s and z_o to be 0.3 m, simulating a moderately strong wind over rough terrain.

Because of the directional nature of the guy properties, the analyses were performed with the wind at two different orientations relative to the structure. As shown in Fig. 6, this included wind parallel to the windward lane of guys (referred as wind at 0°) and wind perpendicular to one face of the mast (referred as wind at 60°); in both cases, the wind vector was aligned parallel to an axis of symmetry of the structure so that out-of-plane static (mean) mast displacements could be avoided. An identical turbulent wind time history was used for both wind directions to facilitate comparisons.

Numerically simulated turbulence time histories were generated for a total of 36 loading points along the mast (i.e. four loading points per mast element). For meaningful results, it was necessary that the resulting storm had spatial and time-varying characteristics that resembled those of the natural wind. Simulated turbulence with prescribed auto-spectrum and cross-spectrum characteristics was generated using a second-order autoregressive process (Iwatani 1982, Reed and Scanlan 1984). A detailed description of the autoregressive wind simulation process used in this study is provided

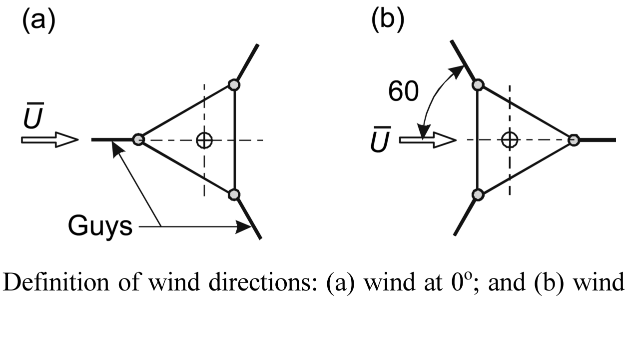

Fig. 6 Definition of wind directions: (a) wind at 0°; and (b) wind at 60°

by Sparling and Davenport (1998). For the finite element analyses, a consistent formulation was used to convert these distributed wind forces into equivalent concentrated forces acting on the mast nodes.

Mean drag forces and aerodynamic damping coefficients associated with the guy nodes were defined as described in Sparling and Davenport (1998). Based on previous studies indicating that fluctuating drag forces acting on the guys did not significantly influence the motion of the mast (Iannuzzi 1986, Peil, *et al*. 1993, Sparling 1995), only mean drag forces were assumed to act on the guys.

4. Analysis results

4.1. Peak guy tension

As the top end of the guy is displaced due to motion of the mast, the corresponding response of the guy is determined by two primary mechanisms. First, the guy adjusts in a quasi-static manner to the change in the position at its top end through a combination of elastic stretching and a change in the amount of sag in its suspended profile. Superimposed on this quasi-static response is the dynamic motion associated with vibration of the guy itself about its quasi-static position. Both

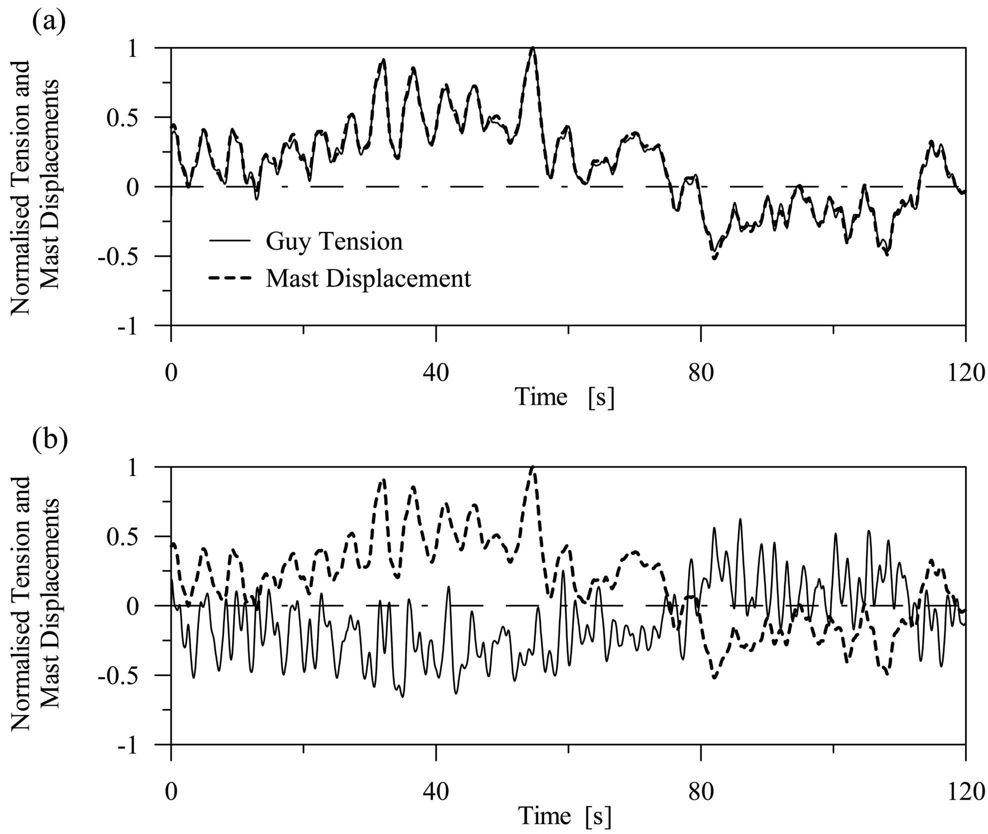

Fig. 7 Comparison of normalised dynamic guy tensions and horizontal mast displacements at the 3rd guy support level (elev. 204.83 m) with the wind at 60°: (a) windward guys; and (b) leeward guy

mechanisms contribute to the dynamic tension fluctuations experienced by the guy (Sparling and Davenport 2000).

Example time history plots of the dynamic (instantaneous less the mean) tension in the windward and leeward guys at the 3rd guy support level are provided in Fig. 7 for the case with the wind at 60°. Plots of the corresponding horizontal mast displacement at that support level are also given. To facilitate comparisons between the two, both the tension and displacement plots have been normalised by their maximum values occurring within the 600 s simulation period.

It is evident that tension fluctuations in the taut windward guys (Fig. 7a) occur largely in unison with the dynamic mast displacements. The high degree of correlation between tension fluctuations and mast displacements in the windward guys suggests that the dynamic tension in these guys can be attributed almost exclusively to the quasi-static response of the guys to imposed displacements at their upper ends.

Dynamic tension fluctuations in the slacker leeward guy (Fig. 7b), on the other hand, are seen to follow the general trend of the dynamic displacement plot, only in an opposite sense (i.e. positive displacements induce negative, or reduced, dynamic tension). However, tension in the leeward guys also exhibits significant additional high frequency content that causes trends in the two plots to differ locally. These high frequency deviations can be attributed to vibration of the guy at its active natural frequencies. Similar observations were made for the guys at other support levels under all wind conditions considered in this study.

The relationship between the dynamic characteristics of the guy tension and mast displacements can also be illustrated by comparing power spectrum plots, as is done in Fig. 8; here, the tension and displacement spectra have been normalised by the mean-square value of the respective

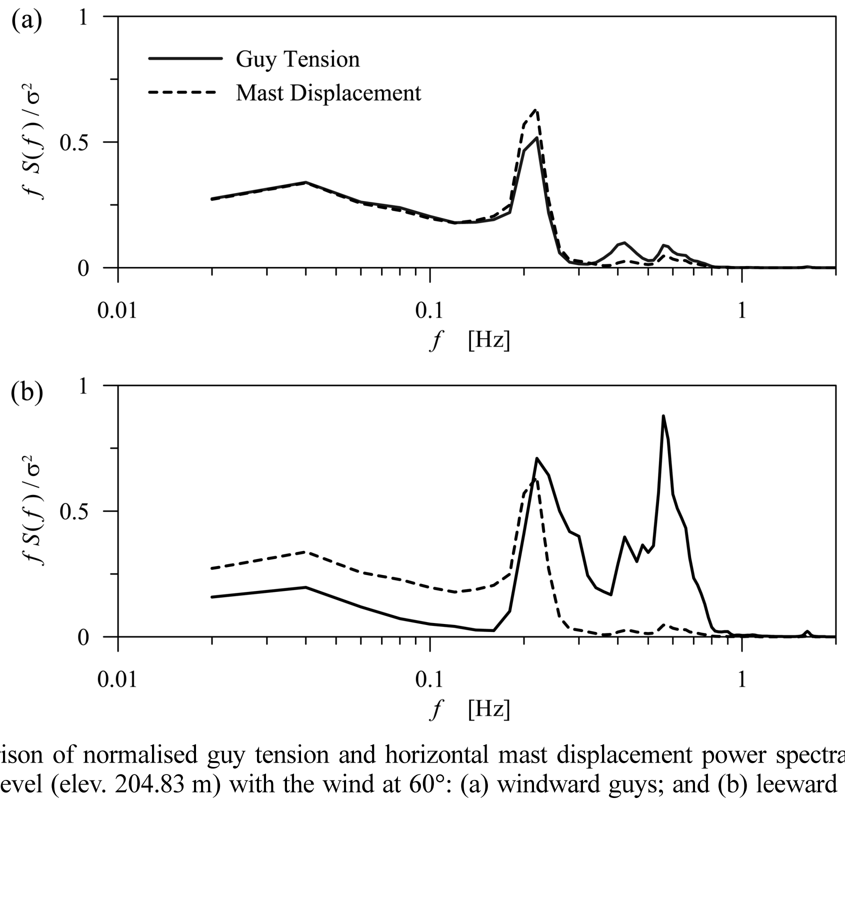

Fig. 8 Comparison of normalised guy tension and horizontal mast displacement power spectra at the 3rd guy support level (elev. 204.83 m) with the wind at 60°: (a) windward guys; and (b) leeward guy

responses, σ^2. As suggested in Fig. 7(a), the frequency content of the dynamic tension and mast displacements is very similar for the windward guys (Fig. 8a), with only slightly elevated tension response levels apparent in the vicinity of the guy's natural frequencies at the higher frequency end of the spectrum. In contrast, the guy tension spectrum for the leeward guy (Fig. 8b) features significant resonant response in the guys, as indicated by the greatly increased high frequency response levels compared to the displacement spectrum, again demonstrating the enhanced role of guy vibrations in generating tension in the slacker leeward cables.

Tension in the taut windward guys will obviously govern strength requirements from a design perspective. Since guy vibrations appear to be of secondary importance in these guys, the quasi-static response of the guys in response to imposed mast displacements will largely determine instantaneous tension values. As a result, the dynamic tension in a windward guy should reach its peak value at the instant the mast at the guy attachment point experiences its peak displacement. In other words, the peak tension should be closely approximated by the quasi-static tension that the guy would experience if its upper end was positioned at the location corresponding to the peak mast displacement. From a practical perspective, this implies that design guy tensions can be estimated statically based on peak dynamic mast displacements calculated using frequency domain methods.

Table 2 summarises the calculated still air, mean, and dynamic guy tension responses for the two wind directions considered in this study. Also included in Table 2 is the static tension that would occur in each of the guys if the peak mast displacement at the corresponding guy attachment point were imposed statically at the guy's upper end.

Table 2. Comparison of static and dynamic guy tension values

Wind Angle	Guy Level [m]	Guy Location	Guy Tension [kN]					
			Still Air	Mean Wind	Dynamic Response			Static at Peak Deflection
					rms	Min.	Max.	
0°	65.76	Windward	94	151	14.2	95	205	204
		Leeward	94	71	5.6	51	93	58
	134.34	Windward	133	241	18.4	184	313	311
		Leeward	133	93	7.0	66	119	76
	204.83	Windward	226	408	26.9	319	516	515
		Leeward	226	164	9.4	132	201	143
	275.310	Windward	142	253	14.7	208	303	306
		Leeward	142	118	5.3	99	136	106
60°	65.76	Windward	94	130	11.1	94	190	190
		Leeward	94	47	9.9	20	96	28
	134.34	Windward	133	202	16.3	159	279	281
		Leeward	133	42	10.3	19	89	27
	204.83	Windward	226	323	21.0	271	422	429
		Leeward	226	95	14.6	52	159	66
	275.310	Windward	142	193	8.4	174	237	237
		Leeward	142	59	11.5	31	102	33

It can be seen that the peak dynamic tensions in the windward guys were reliably predicted by the static tension based on the peak mast displacements, with the peak static and dynamic tension values differing by less than 1.7% in all cases. This finding supports the contention that additional dynamic tension due to guy vibrations need not be considered in the design of the cables for strength.

The minimum dynamic tension in the leeward guys, on the other hand, was found to be overestimated by as much as 42% by the static tension values based on peak mast displacements. While the leeward guys are not critical in terms of the design for strength, the range of dynamic tensions experienced by the leeward guys may nevertheless be of interest for fatigue considerations. Therefore, consideration of guy vibrations may be warranted in design checks for fatigue of the guys and guy hardware, if not for strength.

4.2. Axial force in the mast due to guy reactions

The axial force in the mast comprises the purely static self weight of the mast and all ancillary attachments as well as the time-varying vertical reaction forces from the prestressed guy cables. At any instant, the dynamic component of the axial force at some location in the mast is therefore determined by a summation of the instantaneous vertical reactions from all guys above the point in question. Since the guys at the various support levels exhibit different dynamic characteristics and are each subjected to a unique time history of imposed mast displacements, the resulting vertical reactions exerted by the guys on the mast are not well coordinated. For example, plots of the resultant dynamic vertical guy reaction forces at the lowest and uppermost guy levels are shown in Fig. 9, with the mean values removed to enhance the comparison. The evident lack of correlation in the guy reaction forces at various levels makes it difficult to estimate peak combined axial force values based on frequency domain estimates of the *rms* responses at individual levels alone.

Because of the nonlinear nature of the guy response, particularly in the leeward guys, a rigorous determination of cross-correlation characteristics of the guy reactions at different levels is impractical. The bounds on the potential combined response, however, can be readily established

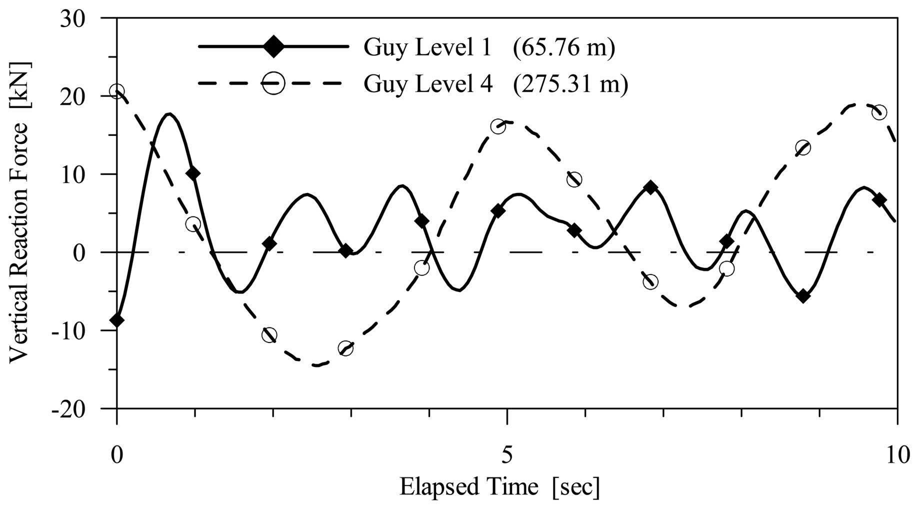

Fig. 9 Dynamic resultant vertical guy reaction forces at the 1st and 4th guy support levels with the wind acting at 0°

from the statistics of the individual guy reactions.

On the one extreme, the individual guy reactions could be completely uncorrelated (statistically independent), allowing the resultant *rms* response to be determined using the square-root-of-the-sum-of-squares (SRSS) combination approach:

$$\tilde{r}_U = \sqrt{\sum_i \tilde{r}_i^2} \tag{6}$$

where $\tilde{r}_U$ is the resultant *rms* response assuming uncorrelated behaviour and $\tilde{r}_i$ is the *rms* fluctuating response of an individual contribution (in this case, the net reaction at one of the guy support levels). On the other extreme, the guy reactions at all levels could be perfectly correlated (acting in complete unison), meaning that the resultant response $\tilde{r}_c$ would be defined by the simple summation:

$$\tilde{r}_C = \sum_i \tilde{r}_i \tag{7}$$

As expected, the resultant *rms* guy reactions calculated from the time series analysis output data fell between the uncorrelated and perfectly correlated bounds described above for both wind directions at all guy levels (Fig. 10a and Fig. 11a). The vertical guy reactions at the different levels were found to exhibit a somewhat higher degree of correlation with the wind at 60° (Fig. 11a) as compared to those with the wind at 0° (Fig. 10a), as indicated by the fact that the calculated resultant reactions were relatively closer to the perfectly correlated values for the 60° case.

Another observation concerning the guyed mast and wind conditions considered in this study was that the fluctuating vertical guy reactions were relatively small compared to the mean, or sustained, component of the response. This is apparent in Fig. 10(b) and Fig. 11(b), which show the total

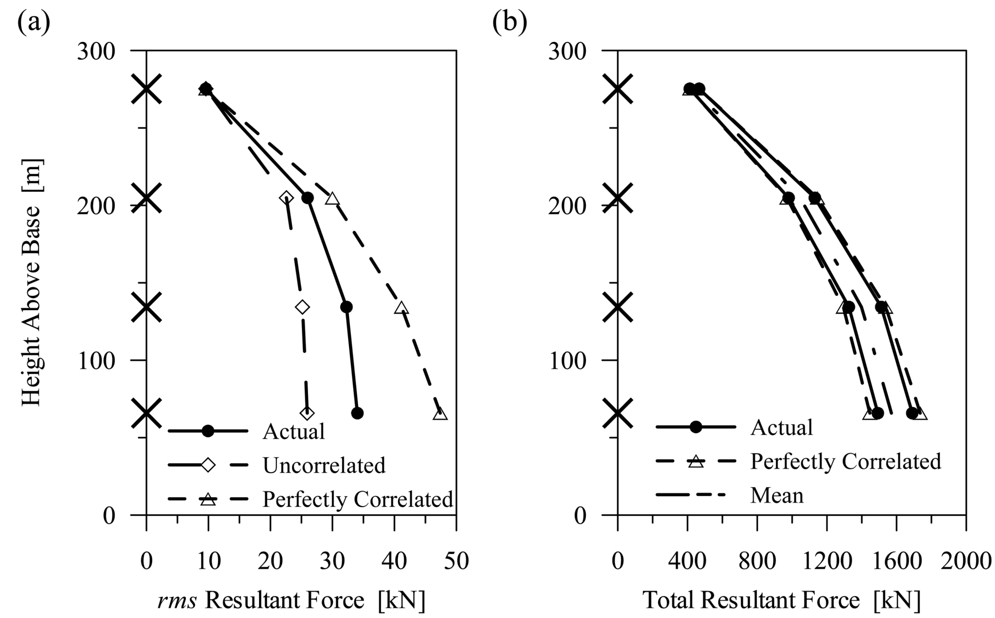

Fig. 10 Resultant vertical guy reactions with the wind at 0° comparing effects of correlation at different guy levels: (a) *rms* guy reactions; and (b) range of total guy reactions

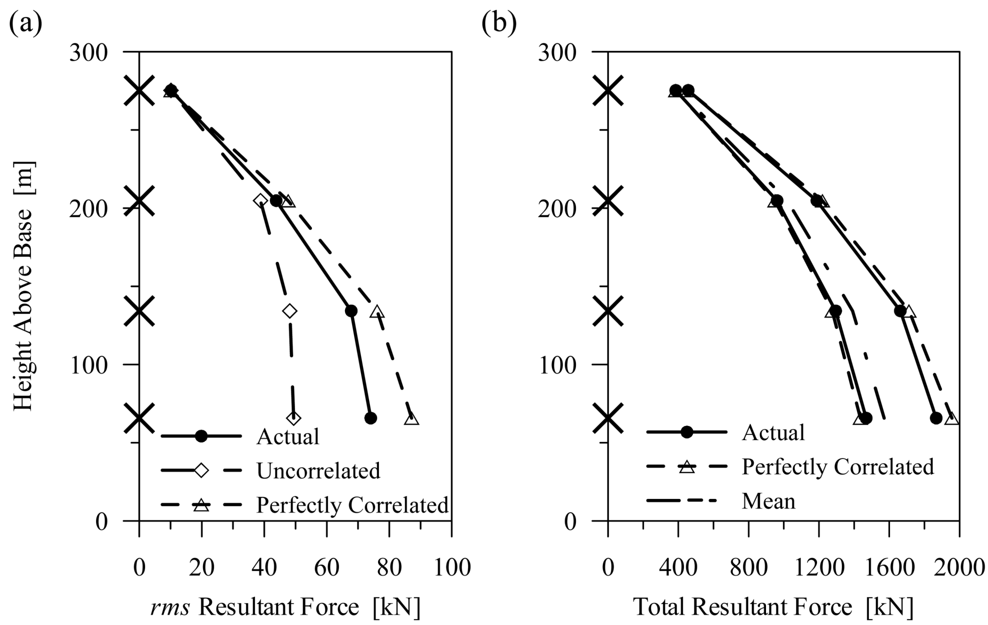

Fig. 11 Resultant vertical guy reactions with the wind at 60° comparing effects of correlation at different guy levels: (a) *rms* guy reactions; and (b) range of total guy reactions

dynamic range of resultant vertical guy reactions at various levels on the mast. For example, the peak dynamic resultant guy reaction near the base of the mast with the wind at 0° is only 7.6% larger than the mean value.

Given the predominance of the mean response component, therefore, the peak resultant guy reaction could be accurately estimated by assuming perfectly correlated behaviour at all guy levels. This would provide an estimate for the peak resultant reaction that overestimated the actual value by less than 2.7%.

With the wind at 60°(Fig. 11b), the fluctuating component of the resultant reaction is somewhat larger, accounting for up to 15.9% of the peak response. In this case, an assumption of perfectly correlated guy reactions at all support levels resulted in estimates of peak resultant vertical guy reactions that were as much as 4.8% higher than the calculated time series values.

Combining the findings relating to guy tension (Section 4.1) and resultant vertical guy reactions presented above, a relatively straightforward procedure for estimating peak axial forces in guyed masts using frequency domain analysis methods can be proposed. First, peak dynamic mast displacements at the guy support levels may be estimated using frequency domain analysis methods. The corresponding peak guy reactions can then be determined from a static analysis of the guys with the corresponding peak mast displacement imposed at their upper end. Finally, an algebraic summation of all peak vertical guy reaction forces, along with the mast self weight, above the point in question will provide a slightly conservative approximation of the peak axial load.

4.3. Mast leg loads

Leg loads in the lattice mast structure arise from the combined actions of axial forces and bending

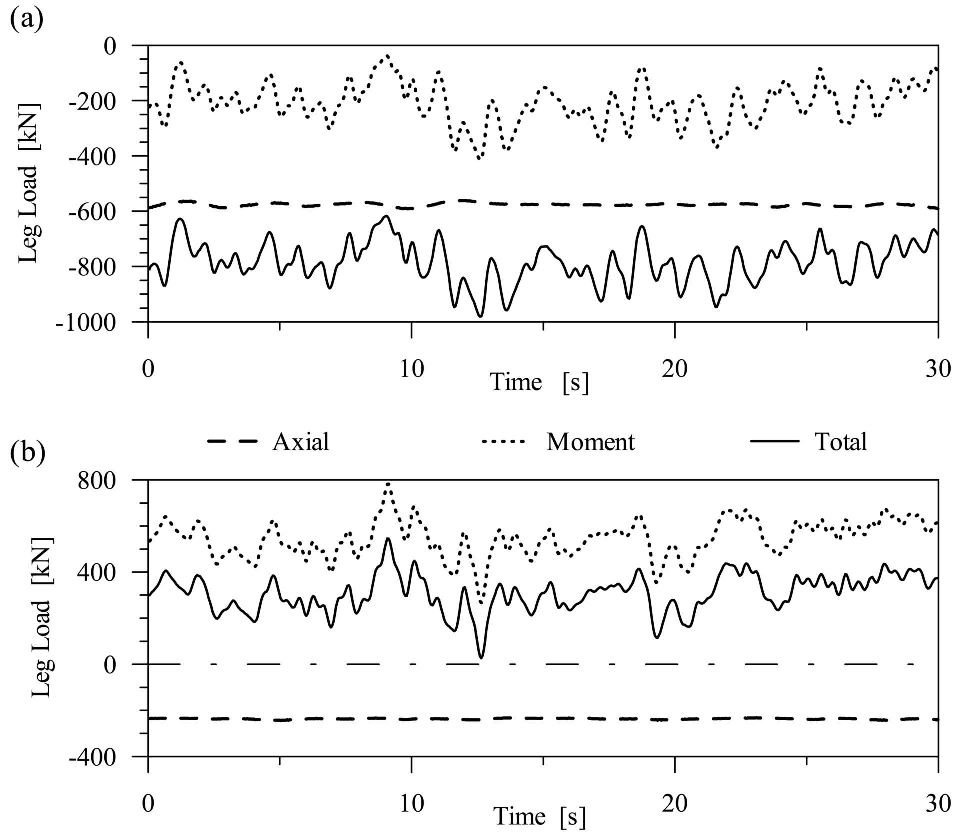

Fig. 12 Time history of leg load components: (a) windward leg at 3rd midspan level (elev. 169.585 m) with wind at 0°; and (b) leeward leg at topmost midspan level (elev. 240.07 m) with wind at 60°.

moments in the mast. To illustrate the relative contributions from these two load effects, example time series plots of the axial load and bending moment leg load components, along with the total instantaneous leg loads, are shown in Fig. 12.

Part (a) of Fig. 12 describes leg loads in the windward leg of the mast at the penultimate midspan location (elevation 169.585 m) with the wind at 0°. Part (b) describes leg loads in the leeward leg at the topmost midspan location (elevation 240.07 m) with the wind at 60°. In both graphs, compressive leg loads are denoted by negative values while tensile loads are positive.

It is obvious from Fig. 12 that dynamic fluctuations in the leg loads arising from bending moments are much larger than leg load fluctuations from axial loads, regardless of the relative magnitude of the two leg load components. Also, the bending moment fluctuations are seen to occur at higher frequencies compared to the slowly varying oscillations of the axial loads.

This second observation can be confirmed by comparing the respective spectral density functions of the bending moments and axial loads, examples of which are shown in Fig. 13. Dynamic axial loads, which arise as a direct result of changes in guy tension due to mast displacements, are dominated by response in the lower vibration modes, while bending moments feature contributions from a number of higher vibration modes. Since random vibration theory implies that peak dynamic responses increase with both the magnitude and frequency of response fluctuations (see Eq. 4), it can be surmised that bending moment fluctuations will dominate the production of peak dynamic leg loads.

In guyed mast analysis models employing some form of "equivalent beam" representation of the mast (Kahla 1993), as opposed to a full space truss model, leg loads must be determined indirectly by combining the load effects produced by bending moments and axial loads in the mast. As

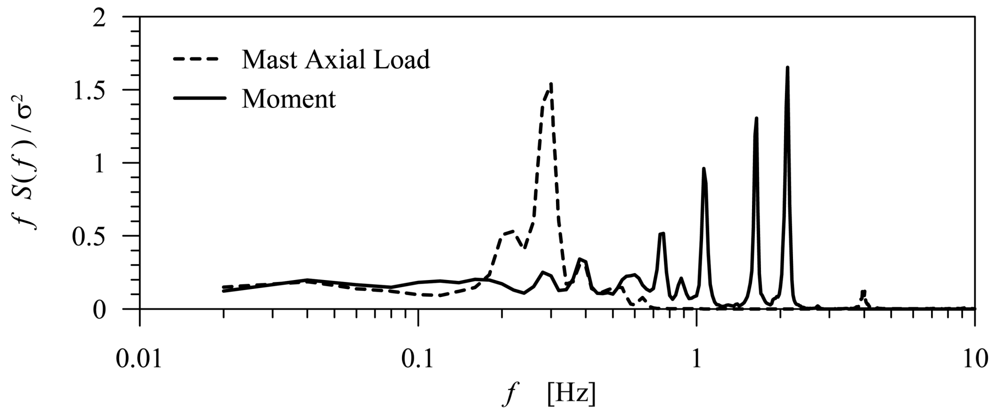

Fig. 13 Normalised power spectra for axial mast loads and bending moments at the 2nd guy support level (elevation 134.34 m) with the wind at 0°

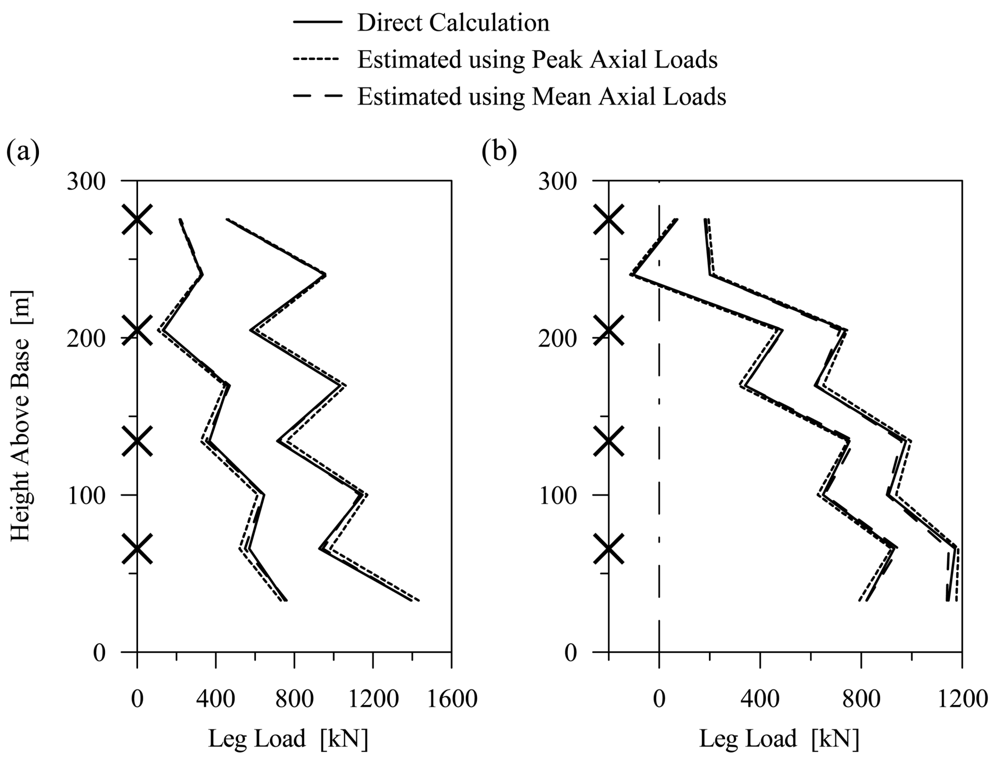

Fig. 14 Comparison of actual and estimated peak leg load ranges with the wind at 0°: (a) windward leg; and (b) leeward leg

discussed previously, the combination of load effects is readily accomplished in time domain analyses since simultaneous moments and axial loads are known explicitly for each time increment. For frequency domain approaches, on the other hand, combining load effects is made difficult by the uncertainty over the degree of correlation that should be assumed between the contributing response components.

Ranges of the peak mast leg loads found in this study are presented in Fig. 14 and Fig. 15 for the cases with the wind at 0° and 60°, respectively. For the sake of comparison, the leg loads calculated directly in the time domain have been compared with two approximate methods used for estimating peak leg loads. In the first approximate method, bending moment and axial force fluctuations were conservatively assumed to be perfectly correlated; therefore, peak leg loads were derived as if the peak bending moment and peak axial load occurred simultaneously at all locations along the mast. In the second approximate method, the dynamic fluctuations in the mast axial force were simply ignored; leg loads in this case were based on peak bending moments and the mean value of the axial force in the mast at the location in question. In effect, the two approximate methods represent upper and lower bounds on potential peak leg load estimates.

In general, there was little significant difference between either of these approximate methods for estimating peak leg loads and the values calculated directly from the time domain output data. Considering both wind directions, the governing compressive leg loads at the various levels in the mast were overestimated by 0.8 - 4.2% when the peak axial mast loads was used in conjunction

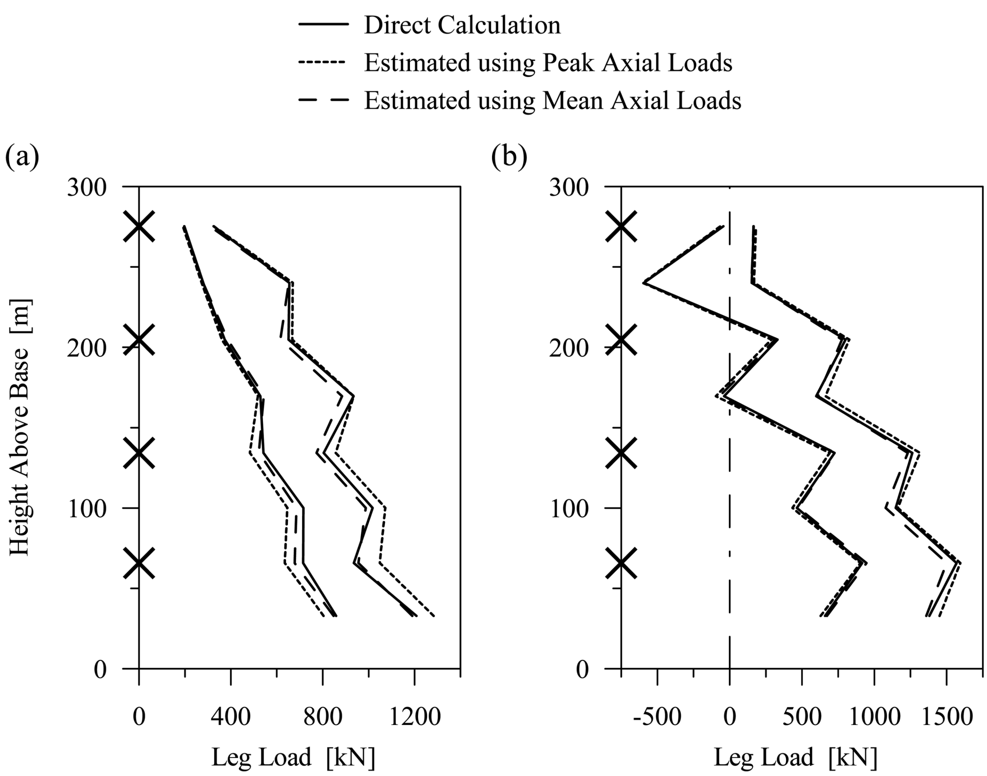

Fig. 15 Comparison of actual and estimated peak leg load ranges with the wind at 60°: (a) windward leg; and (b) leeward leg.

with the peak moments; when using mean axial mast loads, on the other hand, peak compressive leg loads were underestimated by 0.0 - 4.3%. Similarly, governing tensile leg loads in the topmost span of the mast were overestimated by 1.4% when using the minimum axial mast loads in conjunction with the peak moments, and underestimated by 0.2% when using mean axial mast loads. Differences between peak leg load estimates were greatest for the windward leg with wind at 60° (Fig. 15a).

5. Summary and Conclusions

The estimation of peak load effects in guyed masts arising from the combined action of several partially correlated structural responses is complicated by the large number of active vibration modes that are typically present, each of which contributes to different responses in varying degrees. In the frequency domain, resultant dynamic load effects are determined by combining individual response components based on some assumption regarding the degree to which the components are statistically correlated. Although well established techniques exist for linear structures, the appropriate approach for combining load effects in guyed masts is less certain due to the nonlinear behaviour of the guy cables.

A numerical study was therefore undertaken to investigate approximate methods for estimating peak wind-induced load effects in guyed telecommunication masts when using frequency domain dynamic analysis methods. To perform this study, nonlinear response time histories of a 295 m mast subjected to a simulated turbulent wind field were generated in the time domain.

For the mast and wind storm considered in this study, the following trends relating to selected peak load effects were observed.

- The peak dynamic tension in windward guy cables could be reliably approximated in a straightforward, quasi-static manner. A purely static analysis of the guys based on the peak dynamic displaced configuration of the mast produced tension values that were consistently within 2% of corresponding peak dynamic tensions. Vibration of the guy itself did not appear to increase peak tensions except in the non-critical, slackened guys on the leeward side of the mast.
- Peak axial loads in the mast estimated assuming perfectly correlated guy reactions at all guy support levels were found to be reasonably accurate, overestimating actual peak axial loads by less than 5%.
- The assumption that peak bending moments and axial loads occurred simultaneously in the mast resulted in a slight (less than 4.2%) overestimation of governing peak compressive leg loads. On the other hand, ignoring axial force fluctuations and using mean axial force values in conjunction with peak bending moments generated slightly (less than 4.3%) unconservative compressive leg loads. Similarly, governing tensile leg loads were slightly (less than 1.7%) overestimated by using minimum axial loads together with peak moments, and accurately reproduced using mean axial force values.

The recommended procedures offer the advantage that all of the required dynamic responses, including peak mast displacements and bending moments, can be reliably estimated in the frequency domain assuming linear dynamic behaviour, while the nonlinear guy effects can be determined separately based on static analyses. It should be noted, however, that these observations were derived on the basis of a single guyed mast analysed under specific wind conditions. Caution should be used in applying these findings to markedly dissimilar situations.

Aknowledgements

Financial support from the Natural Sciences and Engineering Research Council of Canada (NSERC) is gratefully acknowledged.

References

ANSI/TIA. (2005), *Structural Standards for Steel Antenna Towers and Antenna Supporting Structures (ANSI/TIA 222-G-2005)*, Telecommunications Industry Association (TIA), Arlington, VA.

ASCE (2002), *Dynamic response of lattice towers and guyed masts,* American Society of Civil Engineers Task Committee on the Dynamic Response of Lattice Towers, ASCE Press, Reston, VA.

Bathe, K.J. and Wilson, E.L. (1976), *Numerical Methods in Finite Element Analysis*, Prentice-Hall, Englewood Cliffs, NJ.

Buchholdt, H.A., Moossavinejad, S. and Iannuzzi, A. (1986), "Non-linear dynamic analysis of guyed masts subjected to wind and guy ruptures", *Proc. Inst. Civ. Eng.*, **81**, Paper 9015, 353-395.

CEN. (2006), *European Standard EN 1993-3-1:2006: Eurocode 3 - Design of steel structures - Part 3-1: Towers, masts and chimneys - Towers and masts*, Comité Européan de Normalisation, Brussels.

Chopra, A.K. (1995), *Dynamics of Structures: Theory and Applications to Earthquake Engineering*. Prentice Hall, Englewood Cliffs, NJ.

CSA. (2001), *CAN/CSA-S37-01 (R2006): Antennas, Towers, and Antenna-Supporting Structures*. Canadian Standards Association, Mississauga, Ontario.

Davenport, A.G. (1962), "Response of slender line like structures to a gusty wind", *Proc. Inst. Civ. Eng.*, **23**, 389-408.

Davenport, A.G. (1964), "Note on the distribution of the largest value of a random function with application to gust loading", *Proc. Inst. Civ. Eng.*, **28**, Paper 6739, 187-196.

Davenport, A.G. and Vickery, B.J. (1968), "The response of the Savannah River guyed stack under wind and earthquake action", *Research Report BLWT-5-68*, Boundary Layer Wind Tunnel Laboratory, Univ. of Western Ontario, London, Ont.

Hartmann, A.J. and Davenport, A.G. (1966), "Comparison of the predicted and measured dynamic response of structures to wind (CFPL Tower)", *Engineering Science Research Report ST-4-66*, Univ. of Western Ontario, London, Canada.

Iannuzzi, A. (1986), "Aerodynamic response of a guyed mast: A deterministic approach", *IASS Bulletin*, **89**, 47-59.

Iannuzzi, A. and Spinelli, P. (1989), "Response of a guyed mast to real and simulated wind", *IASS Bulletin*, **99**, 38-45.

IASS. (1981), *Recommendations for Guyed Masts,* International Association for Shell and Spatial Structures, Madrid.

Iwatani, Y. (1982), "Simulation of multidimensional wind fluctuations having any arbitrary power spectra and cross spectra", *J. Wind Eng.*, **11**, 5-18.

Kahla, N.B. (1993), Static and dynamic analysis of guyed towers, Ph.D. Thesis, University of Wisconsin-Madison.

Kärnä, T. (1984), *Dynamic and aeroelastic action of guy cables.* Publication 18, Technical Research Centre of Finland, 91 pp.

Peil, U., Nölle, H. and Wang, Z.H. (1993), "Dynamic behavior of guys", *Proceedings of the Meeting of the IASS Working Group No. 4 on Masts and Towers*, Prague, Sept.

Reed, D.A. and Scanlan, R.H. (1984), "Autoregressive representation of longitudinal, lateral, and vertical turbulence spectra", *J. Wind Eng. Ind. Aerod.*, **17**(2), 199-214.

Sparling, B.F. (1995), *The dynamic behavior of guys and guyed masts in turbulent winds,* Ph.D. Thesis, University of Western Ontario, London, Canada.

Sparling, B.F. and Davenport, A.G. (1998), "Three dimensional dynamic response of guyed towers to wind turbulence", *Can. J. Civ. Eng.*, **25**, 512-525.

Sparling, B.F. and Davenport, A.G. (2000), "The nonlinear dynamic behaviour of guy cables in turbulent winds", *Can. J. Civ. Eng.*, **28**, 98-110.

Sparling, B.F. and Wegner, L.D. (2005), "Comparison of frequency and time domain analyses for guyed masts in turbulent winds", *Can. J. Civ. Eng.*, Accepted for publication.

Vellozzi, J.W. (1975), "Tall guyed tower response to wind loading", *Proceedings of the 4th International Conference on Wind Effects on Buildings and Structures*, London, UK, 735-743.

AK